PHYSICAL REVIEW D **87,** 013011 (2013)

Vacuum polarization and dynamical chiral symmetry breaking: Phase diagram of QED with four-fermion contact interaction

F. Akram,[1] A. Bashir,[2,3,4] L. X. Gutiérrez-Guerrero,[2] B. Masud,[1] J. Rodríguez-Quintero,[5] C. Calcaneo-Roldan,[6] and M. E. Tejeda-Yeomans[6]

[1]*Centre for High Energy Physics, University of the Punjab, Lahore 54590, Pakistan*
[2]*Instituto de Física y Matemáticas, Universidad Michoacana de San Nicolás de Hidalgo, Edificio C-3, Ciudad Universitaria, Morelia, Michoacán 58040, Mexico*
[3]*Physics Division, Argonne National Laboratory, Argonne, Illinois 60439, USA*
[4]*Center for Nuclear Research, Department of Physics, Kent State University, Kent, Ohio 44242, USA*
[5]*Departamento de Física Aplicada, Facultad de Ciencias Experimentales, Universidad de Huelva, Huelva 21071, Spain*
[6]*Departamento de Física, Universidad de Sonora, Boulevard Luis Encinas J. y Rosales, Colonia Centro, Hermosillo, Sonora 83000, Mexico*

(Received 7 September 2012; published 25 January 2013)

We study chiral symmetry breaking for fundamental charged fermions coupled electromagnetically to photons with the inclusion of a four-fermion contact self-interaction term, characterized by coupling strengths α and λ, respectively. We employ multiplicatively renormalizable models for the photon dressing function and the electron-photon vertex that minimally ensures mass anomalous dimension $\gamma_m = 1$. Vacuum polarization screens the interaction strength. Consequently, the pattern of dynamical mass generation for fermions is characterized by a critical number of massless fermion flavors $N_f = N_f^c$ above which chiral symmetry is restored. This effect is in diametrical opposition to the existence of criticality for the minimum interaction strengths, α_c and λ_c, necessary to break chiral symmetry dynamically. The presence of virtual fermions dictates the nature of phase transition. Miransky scaling laws for the electromagnetic interaction strength α and the four-fermion coupling λ, observed for quenched QED, are replaced by a mean field power law behavior corresponding to a second-order phase transition. These results are derived analytically by employing the bifurcation analysis and are later confirmed numerically by solving the original nonlinearized gap equation. A three-dimensional critical surface is drawn in the phase space of (α, λ, N_f) to clearly depict the interplay of their relative strengths to separate the two phases. We also compute the β functions (β_α and β_λ) and observe that α_c and λ_c are their respective ultraviolet fixed points. The power law part of the momentum dependence, describing the mass function, implies $\gamma_m = 1 + s$, which reproduces the quenched limit trivially. We also comment on the continuum limit and the triviality of QED.

DOI: 10.1103/PhysRevD.87.013011 PACS numbers: 12.20.−m, 11.15.Tk, 11.30.Rd

Since the works of Maskawa and Nakajima as well as the Kiev group [1], it is well known that quenched quantum electrodynamics (QED) exhibits vacuum rearrangement, which triggers chiral symmetry breaking when the interaction strength $\alpha = e^2/(4\pi)$ exceeds a critical value $\alpha_c \sim 1$. α_c was argued to be an ultraviolet stable fixed point defining the continuum limit in supercritical QED. Although these works were carried out for the bare vertex in the Landau gauge, principle qualitative conclusions were later shown to be robust even for the most general and sophisticated *Ansätze* put forward henceforth for an arbitrary value of the covariant gauge parameter; see, e.g., Refs. [2–5]. Bardeen *et al.* [6] demonstrated that the composite operator $\bar{\psi}\psi$ acquires large anomalous dimensions at $\alpha = \alpha_c$. In fact, the mass anomalous dimension was shown to be $\gamma_m = 1$, leading to the fact that the four-fermion interaction operator $(\bar{\psi}\psi)^2$ acquires the scaling dimension of $d = 2(3 - \gamma_m) = 4$ instead of 6, and becomes renormalizable. This is an example of when an interaction that is irrelevant in a certain region of phase space (perturbative) might become relevant in another (nonperturbative). Consequently, the four-fermion contact interaction becomes marginal whose absence cannot render QED a closed theory in the strong coupling domain. Depending upon the nonperturbative details of the fermion-boson interaction, it is plausible to have $\gamma_m > 1$, implying $d < 4$, which would modify the status of the four-point operators from marginal to relevant; see, e.g., the review article [7], and references therein. The upshot of the argument is that the robustness of any conclusion about strong QED can be guaranteed only if it is supplemented by these perturbatively irrelevant operators. Quenched QED with the inclusion of these additional operators has been studied in Ref. [8].

Unquenching QED involves inclusion of fermion loops. It provides screening and transforms the vacuum characteristics drastically, changing the Miransky scaling law for the dynamically generated mass $m \sim \Lambda \mathrm{Exp}[-\pi/\sqrt{\alpha/\alpha_c - 1}]$ to a mean field square-root behavior, i.e., $m \sim \Lambda\sqrt{\alpha - \alpha_c}$, [9]. See also Ref. [10] and references therein. Employing a multiplicatively renormalizable photon propagator proposed by Kizilersu and Pennington [11], it has recently been shown that a large value of N_f restores chiral symmetry above a critical value N_f^c, and the corresponding scaling law itself is a square-root: $m \sim \Lambda\sqrt{N_f^c - N_f}$, [12]. However, these results were demonstrated without incorporating four-fermion interactions. In this article, we include this additional interaction and establish the robustness of this result with the inclusion of all the driving elements that influence chiral symmetry breaking, namely, α: the QED interaction strength; λ: the coupling constant related to the four-fermion interactions; and N_f: the fermion flavors whose effect is diametrically opposed to that of α and λ. We study the details of chiral symmetry breaking in the vicinity of the phase change, mapping out the phase space of all these relevant parameters and report the results that survive as well as the ones that get modified in different regimes of this phase transition.

In Sec. I, we introduce the framework of the Schwinger-Dyson equations (SDEs), the notation as well as the assumptions we employ for our analysis. Section II is dedicated to the analytic treatment of the gap equation in the neighborhood of the critical plane that separates chirally symmetric and asymmetric solutions. Next, in Sec. III, we present the results of our numerical analysis. Section IV summarizes our findings and provides an outlook for future work.

I. SDE FOR THE FERMION PROPAGATOR

The starting point for our analysis is the SDE for the electron propagator

$$S^{-1}(p) = S_0^{-1}(p) + ie^2 \int \frac{d^4k}{(2\pi)^4} \gamma^\mu S(k) \Gamma^\nu(k,p) \Delta_{\mu\nu}(q) - iG_0 \int \frac{d^4k}{(2\pi)^4} \mathrm{Tr}[S(k)], \tag{1}$$

where $q = k - p$, e is the electromagnetic coupling and G_0 is the four-fermion coupling. We define the dimensionless four-fermion coupling λ as $\lambda/\Lambda^2 = G_0/(4\pi^2)$. $S_0^{-1}(p) = \not{p}$ is the inverse bare propagator for massless electrons. We parametrize the full propagator $S(p)$ in terms of the electron wave function renormalization $F(p^2)$ and the mass function $M(p^2)$ as $S(p) = F(p^2)/(\not{p} - M(p^2))$. $\Delta_{\mu\nu}(q)$ is the full photon propagator that can be conveniently written as

$$\Delta_{\mu\nu}(q) = -\frac{G(q^2)}{q^2}\left(g_{\mu\nu} - \frac{q_\mu q_\nu}{q^2}\right) - \xi \frac{q_\mu q_\nu}{q^4}, \tag{2}$$

where ξ is the covariant gauge parameter such that $\xi = 0$ corresponds to the Landau gauge. $G(q^2)$ is the photon renormalization function or the dressing function. The full electron-photon vertex is represented by $\Gamma^\mu(k,p)$. The form of the full vertex is tightly constrained by various key properties of the gauge theory [7], e.g., multiplicative renormalizability of the fermion and the gauge boson propagators [2,11,13], perturbation theory [14], the requirements of gauge invariance/covariance [5,15–19], and, of course, observed phenomenology [20]. The most general decomposition of this vertex in terms of its longitudinal and transverse components is

$$\Gamma^\mu(k,p) = \sum_{i=1}^{4} \lambda_i(k,p) L_i^\mu(k,p) + \sum_{i=1}^{8} \tau_i(k,p) T_i^\mu(k,p), \tag{3}$$

where $L_1^\mu = \gamma^\mu$, $L_2^\mu = (k+p)^\mu(\not{k} + \not{p})$, $L_3^\mu = (k+p)^\mu$, and $L_4^\mu = \sigma^{\mu\nu}(k+p)_\nu$, where $\sigma^{\mu\nu} = [\gamma^\mu, \gamma^\nu]/2$. The coefficients λ_i are determined through the Ward-Takahashi identity

$$(k-p)_\mu \Gamma^\mu(k,p) = S^{-1}(k) - S^{-1}(p), \tag{4}$$

relating the electron propagator with the electron-photon vertex [21]. Starting from the limiting form of this identity, namely, the Ward identity,

$$\frac{\partial S^{-1}(p)}{\partial p_\mu} = \Gamma^\mu(p,p), \tag{5}$$

employing the most general form of the fermion propagator and then generalizing to arbitrarily different momenta, one obtains

$$\begin{aligned} \lambda_1(k,p) &= \frac{1}{2}\left[\frac{1}{F(k^2)} + \frac{1}{F(p^2)}\right], \\ \lambda_2(k,p) &= \frac{1}{2}\frac{1}{k^2 - p^2}\left[\frac{1}{F(k^2)} - \frac{1}{F(p^2)}\right], \\ \lambda_3(k,p) &= -\frac{1}{k^2 - p^2}\left[\frac{M(k^2)}{F(k^2)} - \frac{M(p^2)}{F(p^2)}\right], \end{aligned} \tag{6}$$

and $\lambda_4(k,p) = 0$.

It has now been established that the choice of the transverse vertex has observable consequences at the hadronic level, despite the fact that the simple rainbow-ladder truncation is sufficient to reproduce a large body of existing experimental data on pseudoscalar and vector mesons such as their masses, charge radii, decay constants, and scattering lengths, as well as their form factors and the valence quark distribution functions [22–32]. For example, the conundrum of mass difference between opposite parity states can only be explained through corrections to the rainbow ladder truncations [33]; also see the review [34]. In addition to the efforts steered through the continuum studies, attempts have also been initiated in lattice field theory to compute the transverse form factors of the fermion-boson vertex in some simple kinematical regimes [35,36]. Extending these efforts to the entire kinematical space of momenta k^2, p^2, and q^2 is numerically challenging and it may require some time before the results are made available. However, despite the fact that the transverse vertex can have a material effect on hadronic properties and is crucial in maintaining key properties of a quantum field theory, the qualitative behavior of the fermion mass function itself is not significantly sensitive to its details. Therefore, for our purpose, we shall restrict ourselves to the simplest construction (Eq. (8) of Ref. [12]) that, in the quenched limit, renders the ultraviolet behavior of $M(p^2)$ to be

$$M(p^2) \sim (p^2)^{\gamma_m/2-1}, \tag{7}$$

with anomalous mass dimensions $\gamma_m = 1$. This large value makes it mandatory to introduce four-point interactions to ensure self-consistency. With this choice of the full vertex, we obtain, in the massless limit,

$$F(p^2) = \left(\frac{p^2}{\Lambda^2}\right)^\nu, \qquad G(q^2) = \left(\frac{q^2}{\Lambda^2}\right)^s, \tag{8}$$

where $\nu = \alpha\xi/(4\pi)$ and $s = \alpha N_f/(3\pi)$. Near criticality, where the generated masses are small, it is reasonable to assume that the power law solutions for the propagators capture, at least qualitatively, a correct description of chiral symmetry breaking. We choose to study the resulting equation for the mass function in the convenient Landau gauge. Results for any other gauge can be derived by applying the Landau-Khalatnikov-Fradkin transformations [19,37,38] or using a vertex *Ansatz* that effectively incorporates gauge covariance properties in its construction; see e.g., Refs. [2,4,5].

After taking the trace of Eq. (1), carrying out the angular integral, and Wick rotating to Euclidean space, we obtain

$$\begin{aligned} M(p^2) = g(p^2)\int_0^{p^2} dk^2 \frac{k^2}{p^2}\frac{M(k^2)}{k^2+M^2(k^2)} \\ + \int_{p^2}^{\Lambda^2} dk^2 \frac{M(k^2)}{k^2+M^2(k^2)} g(k^2) \\ + \frac{\lambda}{\Lambda^2}\int_0^{\Lambda^2} dk^2 \frac{k^2 M(k^2)}{k^2+M^2(k^2)}, \end{aligned} \tag{9}$$

where $g(p^2) = s_0 G(p^2)$, $s_0 = 3\alpha/(4\pi)$, and Λ is the ultraviolet cutoff that regularizes the integrals. Note that we have employed the simplifying assumption $G(q^2) = G(k^2)$ for $k^2 > p^2$ and $G(q^2) = G(p^2)$ for $p^2 > k^2$, which would allow for the analytic treatment of the linearized equation for the mass function as detailed in the following section.

II. ANALYTIC TREATMENT

Before we venture into the computation of the mass function by numerically solving the above nonlinear integral equation, we find it insightful to make analytical inroads. The differential version of the gap equation (9) simplifies in the neighborhood of the critical coupling α_c; viz., the coupling whereat $M(p^2) \neq 0$ solution bifurcates away from the $M(p^2) = 0$ solution, which alone is possible in perturbation theory. The behavior of the solution near the bifurcation point may be investigated by performing functional differentiation of the gap equation with respect to $M(p^2)$ and evaluating the result at $M(p^2) = 0$. Practically, this amounts to analyzing a linearized form of the original gap equation [i.e., the equation obtained by eliminating all terms of quadratic or higher order in $M(p^2)$],

$$\begin{aligned} M(p^2) = \frac{g(p^2)}{p^2}\int_0^{p^2} dk^2 M(k^2) + \int_{p^2}^{\Lambda^2} dk^2 \frac{M(k^2)}{k^2} g(k^2) \\ + \frac{\lambda}{\Lambda^2}\int_0^{\Lambda^2} dk^2 M(k^2). \end{aligned} \tag{10}$$

Note that the nonlinearized version of this equation receives negligible contribution from the region $k^2 \to 0$, while this is not true for Eq. (10). This shortcoming is readily remedied by introducing an infrared cutoff m^2 such that $M(m) = m$. The resultant linearized gap equation, Eq. (10), can now be studied analytically in the neighborhood of the critical plane on converting it into a second-order linear differential equation

$$x^2 M''(x) + sxM'(x) + s_0(1-s)\frac{M(x)}{x^s} = 0, \tag{11}$$

with two boundary conditions. Here we have used the convenient substitution $x = \Lambda^2/p^2$. Following are the infrared and ultraviolet boundary conditions

$$M'(\Lambda^2/m^2) = 0, \tag{12a}$$

$$M(1) = \left(1+\frac{\lambda}{s_0}\right)\frac{M'(1)}{1-s}. \tag{12b}$$

Note that the four-fermion coupling only affects the ultraviolet boundary condition. The differential equation itself and the infrared boundary condition do not have any direct dependence on it. It is what we expect intuitively. A four-fermion Nambu—Jona-Lasinio type term only generates a constant mass term. Therefore, it effectively serves as a cutof-dependent bare mass and can hence only influence the dynamics through the ultraviolet boundary condition.

If we now apply the Lommel transformations, $z = Bx^\gamma$ and $W(x) = x^{-a}M(x)$, the linearized equation can be converted into the following Bessel differential equation:

$$z^2 W''(z) + zW'(z) + (z^2 - A^2)W(z) = 0, \tag{13}$$

where $\gamma = -s/2$, $a = (1-s)/2$, $A = (1-s)/s$, and $B = \sqrt{3\alpha(1-s)/(\pi s^2)}$, where $s < 1$. The boundary conditions in terms of the function $W(z)$ are given by

$$aW(z) + \gamma z W'(z)|_{z=B(m/\Lambda)^s} = 0, \tag{14a}$$

$$a(s_0-\lambda)W(z) - \gamma z(s_0+\lambda)W'(z)|_{z=B} = 0. \tag{14b}$$

The general solution of the second-order differential equation (13) is

$$W(z) = c_1 J_A(z) + c_2 Y_A(z), \tag{15}$$

where $J_A(z)$ and $Y_A(z)$ are the Bessel functions of the first and the second kind, respectively. The power law part of momentum dependence of the mass function $M(x) = x^a W(x)$ is neatly separated out into the factor x^a, implying $\gamma_m = 1 + s$. Note that $s = 1$ corresponds to a *momentum-independent* photon propagator that implies $\gamma_m = 2$. Consequently, Eq. (7) implies that it corresponds to a momentum-independent mass function, a result that is readily and analytically confirmed from the resultant simple integral equation. This is a well-known behavior of a contact interaction model of the Nambu—Jona-Lasinio type. Moreover, the quenched limit of $\gamma_m = 1$ is also reproduced trivially.

For the homogenous boundary conditions of Eqs. (14), the nontrivial chirally asymmetric solution of the gap equation exists if the following condition holds:

$$\left[\frac{2aJ_A(z) + \gamma z(J_{A-1}(z) - J_{A+1}(z))}{2aY_A(z) + \gamma z(Y_{A-1}(z) - Y_{A+1}(z))}\right]_{z=B(m/\Lambda)^s} = \frac{(1+\lambda/s_0)\gamma B(J_{A-1}(B) - J_{A+1}(B)) - (1-s)(1-\lambda/s_0)J_A(B)}{(1+\lambda/s_0)\gamma B(Y_{A-1}(B) - Y_{A+1}(B)) - (1-s)(1-\lambda/s_0)Y_A(B)}. \tag{16}$$

In the limit of $\Lambda \to \infty$, we obtain the following result for the dynamically generated mass m:

$$\frac{m^2}{\Lambda^2} \equiv f(\alpha, N_f, \lambda) = \left[\frac{2}{B}\right]^{\frac{2}{s}} \frac{\Gamma(A)\Gamma(A+2)2a}{\pi\gamma}\left[\frac{(1+\lambda/s_0)\gamma B(J_{A-1}(B) - J_{A+1}(B)) - (1-s)(1-\lambda/s_0)J_A(B)}{(1+\lambda/s_0)\gamma B(Y_{A-1}(B) - Y_{A+1}(B)) - (1-s)(1-\lambda/s_0)Y_A(B)}\right]. \tag{17}$$

Carrying out the Taylor expansion near the critical point, we find the following scaling laws:

$$\frac{m}{\Lambda} = A_1(\lambda, N_f)[\alpha - \alpha_c(\lambda, N_f)]^{1/2}, \tag{18}$$

$$\frac{m}{\Lambda} = A_2(\alpha, N_f)[\lambda - \lambda_c(\alpha, N_f)]^{1/2}, \tag{19}$$

$$\frac{m}{\Lambda} = A_3(\alpha, \lambda)[N_f^c(\alpha, \lambda) - N_f]^{1/2}. \tag{20}$$

The exact form of the functional dependence of A_i, α_c, λ_c, and N_f^c on the relevant pair of α, λ, and N_f can be derived from Eq. (17) but, not yielding novel insight into the problems at hand, we refrain from computing it. The momentum dependence of the mass function (based upon the numerical calculation discussed in the next section) and the scaling laws for λ, α, and N_f have been plotted in Figs. 1–5.

The critical values of the parameters α, N_f, and λ define a surface in the 3D phase space of these parameters. The mass function is zero (nonzero) below (above) the critical surface, which corresponds to restored (broken) chiral symmetry. The analytic expression for the critical surface can be obtained by setting $m/\Lambda = 0$ in Eq. (17). The resultant equation, which can be solved for λ, is given by

$$\lambda = -s_0\frac{[\gamma B(J_{A-1}(B) - J_{A+1}(B)) - (1-s)J_A(B)]}{[\gamma B(J_{A-1}(B) - J_{A+1}(B)) + (1-s)J_A(B)]}. \tag{21}$$

In order to obtain a finite mass for the charged fermion in the limit of $\Lambda \to \infty$, one requires charge renormalization. Therefore, in this limit, we impose $\alpha(\Lambda) = \alpha_c + m^2/(A^2\Lambda^2)$. One can thus readily obtain the corresponding β function,

$$\beta_\alpha = \Lambda\frac{\partial\alpha}{\partial\Lambda}\bigg|_{\lambda, N_f} = -2(\alpha - \alpha_c). \tag{22}$$

Therefore, α_c is the ultraviolet fixed point of β_α, as has been observed in Ref. [9]. Identical presence of the fixed point for β_λ for λ_c is readily observed:

$$\beta_\lambda = \Lambda\frac{\partial\lambda}{\partial\Lambda}\bigg|_{\alpha, N_f} = -2(\lambda - \lambda_c). \tag{23}$$

Note that we have restricted ourselves to the mean field approach, i.e., we work within the approximations that neglect quantum corrections corresponding to four-fermion interactions beyond the tree level. Taking into account these corrections is beyond the scope and the

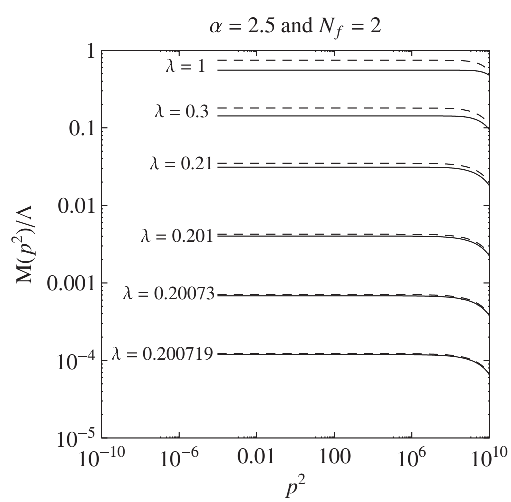

FIG. 1. The mass functions for different values of λ at fixed $\alpha = 2.5$ and $N_f = 2$. Its increasing sensitivity to the variation in lambda helps locate the critical strength λ_c. Dashed and solid curves represent mass functions with [vacuum polarization of Eq. (25)] and without feedback [vacuum polarization of Eq. (8)] from the gap equation, respectively.

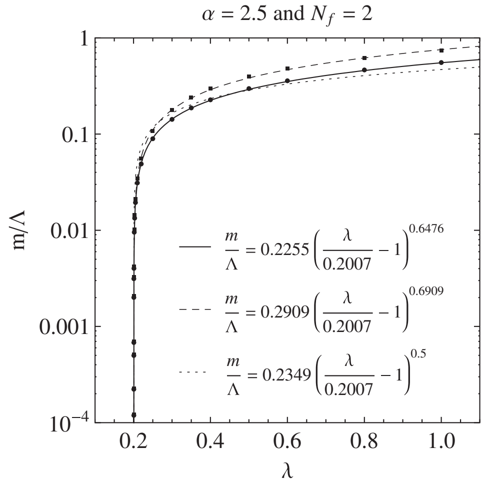

FIG. 2. The scaling law for four-fermion coupling λ. Dotted, solid, and dashed lines represent numerical results, fit to the numerical data with a power law, and analytically predicted square-root scaling law, respectively, at $\alpha = 2.5$ and $N_f = 2$. The mean field behavior of the chiral phase transition is evident. Dashed and solid curves represent mass functions with [vacuum polarization of Eq. (25)] and without feedback [vacuum polarization of Eq. (8)] from the gap equation, respectively.

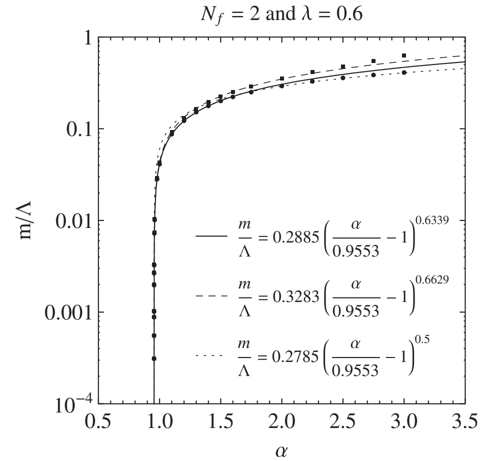

FIG. 4. The scaling law for the coupling α, investigated through the behavior of the mass function near criticality, Fig. 3. Dotted, solid, and dashed lines represent numerical results, fit of the numerical data to the power law, and analytically predicted square-root scaling law, respectively, at $N_f = 2$ and $\lambda = 0.6$. Dashed and solid curves represent mass functions with [vacuum polarization of Eq. (25)] and without feedback [vacuum polarization of Eq. (8)] from the gap equation, respectively.

thrust of this article. Having said that, going beyond our approximation would require incorporating the SDE for the full Green function corresponding to the four-fermion degrees of freedom. One way of achieving this at the level of the Bethe-Salpeter fermion-antifermion scattering kernel is the skeleton expansion. Another way of incorporating this is the Cornwall-Jackiw-Tamboulis effective potential written in terms of the composite degrees of freedom for higher loops; see for example Ref. [39]. For the four-fermion interaction part, the conclusions obtained in Ref. [39] are the same as ours, i.e., there is an ultraviolet fixed point whose quantitative form along the critical curve

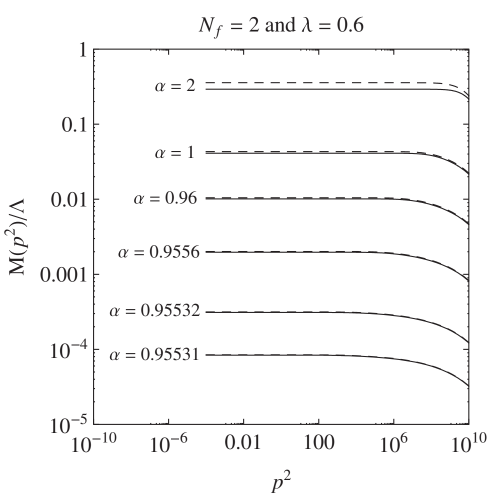

FIG. 3. The mass function $M(p^2)$ for varying values of the electromagnetic coupling α for fixed values of massless fermion flavors $N_f = 2$ and the four-fermion coupling $\lambda = 0.6$. The objective is to hunt α_c and determine the nature of the phase transition. Dashed and solid curves represent mass functions with [vacuum polarization of Eq. (25)] and without feedback [vacuum polarization of Eq. (8)] from the gap equation, respectively.

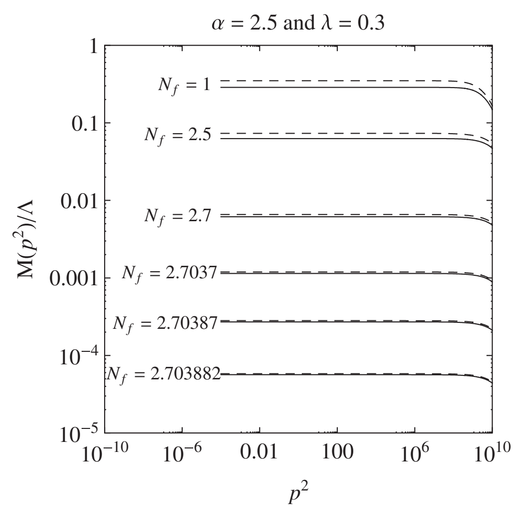

FIG. 5. The mass function $M(p^2)$ for increasing number of massless fermion flavors diminishes because the interaction gets screened. Chiral symmetry is restored above a certain N_f^c, which depends upon the values of α and λ. Dashed and solid curves represent mass functions with [vacuum polarization of Eq. (25)] and without feedback [vacuum polarization of Eq. (8)] from the gap equation, respectively.

is the same as given by Eq. (23). As pointed out before, the critical value λ_c has a functional dependence on α. The work of Kondo *et al.* suggests that, at least when we restrict ourselves to the immediate neighborhood of the critical curve, λ_c captures all the dependence on α, even on including four-fermion interactions.

The analytical results of this section can be confirmed and made precise through a numerical study of the nonlinearized gap equation (9). This analysis is presented in the next section.

III. NUMERICAL RESULTS

In order to compare and confirm the above analytical results, based on the linearized approximation, we solve the original nonlinear integral equation (9) numerically for varying N_f, α, and λ. Depicted in Fig. 1 is the fermion mass functions for different values of λ for $\alpha = 2.5$ and $N_f = 2$. The closer we get to the critical value λ_c, the more drastically pronounced is the drop in the mass function, indicating the approaching onslaught of the phase transition. The scaling law is explored in Fig. 2, where the variation of $m/\Lambda \equiv M(p^2 = 0)/\Lambda$ with λ is plotted at the fixed values of α and N_f. The fit of the complete numerical data shows that the power of the scaling law is slightly different from 0.5. This is expected as the mean field scaling behavior (20) captures the correct physics only in the immediate vicinity of the critical point where the linearized version of the equation becomes exact. In the same figure, we also superimpose the analytically derived square-root scaling law that, as expected, sits exactly atop the numerical findings in the immediate vicinity of the critical point. In Figs. 3 and 4, we show the variation of the mass section and the corresponding scaling law as a function of α at fixed values of $N_f = 2$ and $\lambda = 0.6$. These results again confirm the validity of the square-root dependence of the dynamically generated mass on the electromagnetic coupling. In Figs. 5 and 6, we plot the mass function in the presence of increasing types of virtual fermion—antifermion pairs and the resulting scaling law as a function of N_f, respectively, for $\alpha = 2.5$ and $\lambda = 0.3$. These results establish the robustness of the conclusions presented in Ref. [12] on the inclusion of the four-point contact interaction term.

Shown in Fig. 7 is the critical curve in the $\lambda - \alpha$ plane at $N_f = 2$. The dynamical mass ceases to exist for the values of λ and α below the curve. The dots in this figure represent the points obtained by numerically solving the nonlinear integral equation of the mass function, and the solid curve represents the analytical result that corresponds to expression (21). This criticality should be considered as an extension of its quenched QED counterpart obtained in Ref. [40]. For the sake of completeness, in Figs. 8 and 9, we present the critical curves in the $\lambda - N_f$ and $\alpha - N_f$ planes for fixed values of $\alpha = 2$ and $\lambda = 0.3$, respectively.

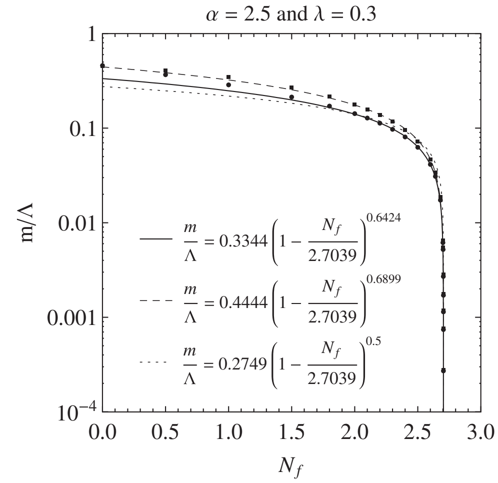

FIG. 6. The scaling law for N_f. Dotted, solid, and dashed lines represent numerical results, fit of the numerical data to the power law, and analytically predicted square-root scaling law, respectively, at $\alpha = 2.5$ and $\lambda = 0.3$. Thus the nature of this transition is independent of the inclusion of the four-fermion interaction term. Dashed and solid curves represent mass functions with [vacuum polarization of Eq. (25)] and without feedback [vacuum polarization of Eq. (8)] from the gap equation, respectively.

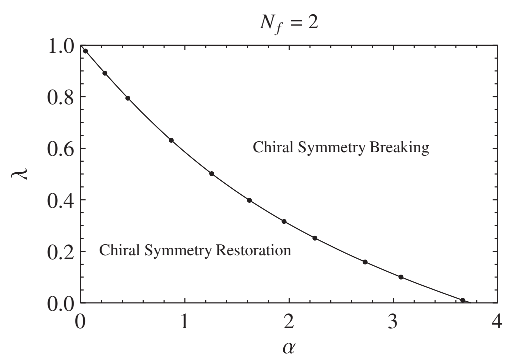

FIG. 7. Critical curve in $\lambda - \alpha$ plane at $N_f = 2$. Dotted and solid curves represent the numerical results and analytical findings, respectively. For a fixed N_f, a chiral symmetry breaking phase is achieved when the combined strength of α and λ lies above the criticality curve, dictated by Eq. (21). The curve is indistinguishable, independently of the photon propagator employed [i.e., Eq. (8) or Eq. (25)]. The same is true for Figs. 8–10.

These figures show that the analytical results agree with the numerical findings with a very good accuracy. Figure 9 gives a quantitative picture of how the growing number of fermion flavors requires a stronger electromagnetic coupling to break chiral symmetry. The relation is not linear. The screening effect exhausts the strength of the interaction faster with increasing N_f.

Finally, in Fig. 10, we present the full critical surface in the phase space of N_f, α, and λ. In the limit of $N_f \to 0$, the Miransky scaling law is reproduced. The results presented in this paper are qualitatively robust if, instead of the

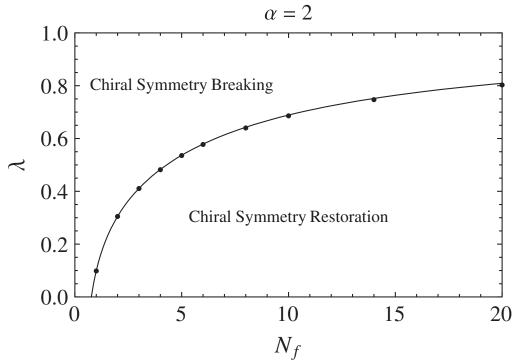

FIG. 8. Critical curve in $\lambda - N_f$ plane at $\alpha = 2$. Dotted and solid curves represent the numerical results and analytical findings, respectively. It is clear that the bifurcation analysis provides an exact analysis of the nonlinear equation at criticality.

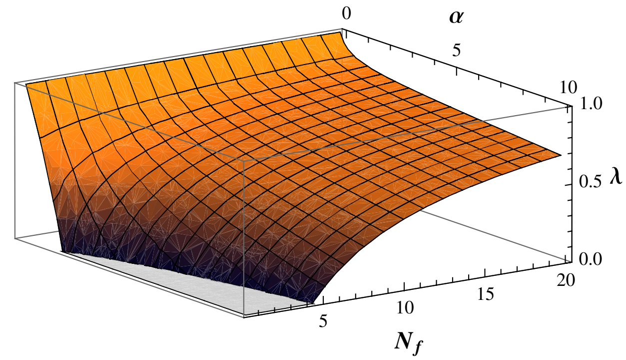

FIG. 10 (color online). A three-dimensional view of the criticality surface. It corresponds to Eq. (21) as well as the numerical analysis of the nonlinearized Eq. (9). The region below the surface represents a chirally symmetric phase.

multiplicatively renormalizable photon propagator of Eq. (8), we employ any of the following models:

(i) One-loop perturbative photon propagator, as employed in Ref. [9]:

$$G(q^2) = 1 + \frac{\alpha N_f}{3\pi} \ln\left(\frac{q^2}{\Lambda^2}\right). \tag{24}$$

(ii) A photon propagator that receives feedback from the gap equation, i.e.,

$$G(q^2) = [(q^2 + M^2(0))/\Lambda^2]^s, \tag{25}$$

which is also multiplicatively renormalizable. For a comparison, we have also displayed numerical results for this latter choice in all the relevant figures. As we had anticipated, near criticality, results are practically indistinguishable from the ones obtained using the model of Eq. (8).

Note that away from criticality, a complete self-consistent coupled solution of the photon and the fermion propagator will be required. However, finiteness of the dynamically generated mass for $\Lambda \to \infty$ forces nonperturbative QED to be consistently defined only for those values of α and λ that lie on the critical surface. This is a simple corollary of the argument laid out in Ref. [6]. Note that as we employ a model for the vacuum polarization, the running coupling is not our prediction. Following Rakow [41], if we define the renormalization at $q^2 = 0$ rather than on the mass shell, we get

$$\alpha_R(0) = \alpha F_R^2(0) G_R(0) = \alpha G_R(0), \tag{26}$$

because $F_R(0) = 1$ for us. Therefore, our model conforms to $\alpha_R(0) \to 0$ in accordance with the lattice computation of unquenched QED [41]. As we have argued before, when $\Lambda \to \infty$, $\alpha \to \alpha_c$. Thus $\alpha_R(0) = \alpha_c G_R(0) \to 0$, which is associated with the triviality of QED in Ref. [41]. We use this same model for the vacuum polarization even in the presence of the perturbatively irrelevant four-fermion interaction terms. This means that on the phase boundary, the renormalized coupling is zero even in the presence of the four-fermion interactions. This is in accordance with the argument presented in Ref. [10]. However, note that for the practical solution of the gap equation, the photon propagator or the running coupling below $q^2 = \kappa^2 = M^2(\kappa^2)$ has no bearing on the chiral symmetry breaking solution.

We now recall that the Bethe-Salpeter equation gives us an approximate relation between the integral over the mass function and the "decay constant of the pion (f)" given by Eq. (4.42) of Ref. [10]

$$f^2 = \int^\Lambda dp^2 p^2 M(p^2) \frac{[M(p^2) - p^2 M'(p^2)/2]}{[p^2 + M^2(p^2)]^2}. \tag{27}$$

We numerically evaluate f for varying values of s and find that $f \to \infty$ in the limit when the ultraviolet regulator $\Lambda \to \infty$, a result that suggests that the continuum limit is the one of noninteracting bosons, in agreement with earlier findings [9,42].

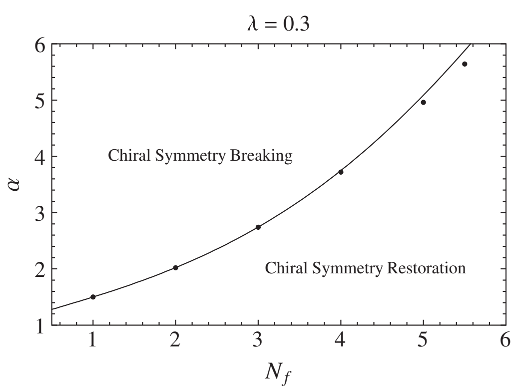

FIG. 9. Critical curve in $N_f - \alpha$ plane at $\lambda = 0.3$. As in the other curves, dots are numerical solutions whereas the solid line is the outcome of the bifurcation analysis.

IV. EPILOGUE

We have studied chiral symmetry breaking for fundamental fermions interacting electromagnetically with photons and self-interacting through perturbatively irrelevant four-fermion contact interaction that is required to render QED a closed theory in its strongly coupled regime, where this additional interaction becomes marginal and, perhaps, even relevant. We have used multiplicatively renormalizable models for the photon propagator (with and without the feedback from the gap equation) that, we argue, should capture the qualitative physics correctly in the vicinity of the critical surface in the phase space of (α, λ, N_f), marking the onslaught of chiral symmetry breaking (restoration). The presence of virtual fermion-antifermion pairs changes the nature of the phase transitions along the α and λ axes. The Miransky scaling law softens down to a square-root mean field scaling behavior as a function of all the three parameters α, λ, and N_f, (20). Study of the mass anomalous dimensions for QED with a model vacuum polarization reveals how, quantitatively, the momentum dependence of the photon propagator, i.e., $(p^2)^{s-1}$, filters into the momentum dependence of the fermion mass function, namely, $(p^2)^{(s-1)/2}$, through the gap equation. We believe that our analysis can and should be extended to the study of QCD through its SDEs. The situation is ripe for the application of this line of approach and technology to QCD, where we are finally having the first glimpses of the flavor dependence of the gluon propagator in the infrared region [43]. This is for future study.

ACKNOWLEDGMENTS

A. B. acknowledges CIC (UMICH) and CONACyT Grants No. 4.10, No. 46614-I, No. 128534, and No. 94527 (Estancia de Consolidación) and the U.S. Department of Energy, Office of Nuclear Physics, Contract No. DE-AC02-06CH11357. We thank V. Gusynin, A. Kızılersü, and C. D. Roberts for useful discussions.

[1] T. Maskawa and H. Nakajima, Prog. Theor. Phys. **52**, 1326 (1974); P. I. Fomin and V. A. Miransky, Phys. Lett. **64B**, 166 (1976); P. I. Fomin, V. P. Gusynin, and V. A. Miransky, Phys. Lett. **78B**, 136 (1978).

[2] D. C. Curtis and M. R. Pennington, Phys. Rev. D **42**, 4165 (1990).

[3] D. Atkinson, J. C. R. Bloch, V. P. Gusynin, M. R. Pennington, and M. Reenders, Phys. Lett. B **329**, 117 (1994).

[4] A. Bashir, A. Raya, and S. Sánchez-Madrigal, Phys. Rev. D **84**, 036013 (2011).

[5] A. Bashir, R. Bermudez, L. Chang, and C. D. Roberts, Phys. Rev. C **85**, 045205 (2012).

[6] W. A. Bardeen, C. N. Leung, and S. T. Love, Phys. Rev. Lett. **56**, 1230 (1986); C. N. Leung, S. T. Love, and W. A. Bardeen, Nucl. Phys. **B273**, 649 (1986).

[7] A. Bashir and A. Raya, *Trends in Boson Research*, edited by A. V. Ling (Nova Science Publishers, New York, 2005).

[8] E. V. Gorbar and E. Sausedo, Ukr. Phys. J. **36**, 1025 (1991); M. Reenders, Ph.D., Groningen University, 1999.

[9] K. Kondo, Y. Kikukawa, and H. Mino, Phys. Lett. B **220**, 270 (1989); V. P. Gusynin, Mod. Phys. Lett. A **05**, 133 (1990).

[10] C. D. Roberts and A. G. Williams, Prog. Part. Nucl. Phys. **33**, 477 (1994).

[11] A. Kizilersu and M. R. Pennington, Phys. Rev. D **79**, 125020 (2009).

[12] A. Bashir, C. Calcaneo-Roldan, L. X. Gutiérrez-Guerrero, and M. E. Tejeda-Yeomans, Phys. Rev. D **83**, 033003 (2011).

[13] Z. Dong, H. J. Munczek, and C. D. Roberts, Phys. Lett. B **333**, 536 (1994); A. Bashir, A. Kizilersu, and M. R. Pennington, Phys. Rev. D **57**, 1242 (1998).

[14] A. Kizilersu, M. Reenders, and M. R. Pennington, Phys. Rev. D **52**, 1242 (1995); A. Bashir, A. Kizilersu, and M. R. Pennington, Phys. Rev. D **62**, 085002 (2000); A. Bashir and A. Raya, Phys. Rev. D **64**, 105001 (2001).

[15] J. C. Ward, Phys. Rev. **78**, 182 (1950); H. S. Green, Proc. Phys. Soc. London Sect. A **66**, 873 (1953); Y. Takahashi, Nuovo Cimento **6**, 371 (1957).

[16] A. Bashir and M. R. Pennington, Phys. Rev. D **50**, 7679 (1994).

[17] A. Bashir and M. R. Pennington, Phys. Rev. D **53**, 4694 (1996).

[18] L. D. Landau and I. M. Khalatnikov, Zh. Eksp. Teor. Fiz. **29**, 89 (1955) [Sov. Phys. JETP **2**, 69 (1956)]; E. S. Fradkin, Sov. Phys. JETP **2**, 361 (1956); K. Johnson and B. Zumino, Phys. Rev. Lett. **3**, 351 (1959).

[19] A. Bashir, Phys. Lett. B **491**, 280 (2000); A. Bashir and A. Raya, Phys. Rev. D **66**, 105005 (2002).

[20] L. Chang and C. D. Roberts, Phys. Rev. Lett. **103**, 081601 (2009).

[21] J. S. Ball and T.-W. Chiu, Phys. Rev. D **22**, 2542 (1980).

[22] P. Maris and C. D. Roberts, Phys. Rev. C **56**, 3369 (1997).

[23] P. Maris and P. C. Tandy, Phys. Rev. C **62**, 055204 (2000).

[24] P. Maris and P. C. Tandy, Phys. Rev. C **65**, 045211 (2002).

[25] C.-R. Ji and P. Maris, Phys. Rev. D **64**, 014032 (2001).

[26] P. Maris and P. C. Tandy, Phys. Rev. C **60**, 055214 (1999).

[27] D. Jarecke, P. Maris, and P. C. Tandy, Phys. Rev. C **67**, 035202 (2003).

[28] P. Maris, PiN Newslett. **16**, 213 (2002).

[29] S. R. Cotanch and P. Maris, Phys. Rev. D **66**, 116010 (2002).

[30] L. X. Gutiérrez-Guerrero, A. Bashir, I. C. Clöet, and C. D. Roberts, Phys. Rev. C **81**, 065202 (2010).

[31] H. L. L. Roberts, C. D. Roberts, A. Bashir, L. X. Gutiérrez-Guerrero, and P. C. Tandy, Phys. Rev. C **82**, 065202 (2010).

[32] T. Nguyen, A. Bashir, C. D. Roberts, and P. C. Tandy, Phys. Rev. C **83**, 062201 (2011).
[33] L. Chang and C. D. Roberts, Phys. Rev. Lett. **103**, 081601 (2009).
[34] A. Bashir, L. Chang, I. C. Cloet, B. El-Bennich, Y.-X. Liu, C. D. Roberts, and P. C. Tandy, Commun. Theor. Phys. **58**, 79 (2012).
[35] J.-I. Skullerud, P. O. Bowman, A. Kizilersu, D. B. Leinweber, and A. G. Williams, J. High Energy Phys. 04 (2003) 047.
[36] A. Kizilersu, D. B. Leinweber, J.-I. Skullerud, and A. G. Williams, Eur. Phys. J. C **50**, 871 (2007).
[37] A. Bashir and R. Delbourgo, J. Phys. A **37**, 6587 (2004); A. Bashir and A. Raya, Nucl. Phys. **B709**, 307 (2005); Few-Body Syst. **41**, 185 (2007); A. Bashir and A. Raya, AIP Conf. Proc. **1026**, 115 (2008); A. Bashir and A. Raya, J. Phys. Conf. Ser. **37**, 90 (2006).
[38] A. Bashir, A. Raya, S. Sánchez-Madrigal, and C. D. Roberts, Few-Body Syst. **46**, 229 (2009).
[39] K.-I. Kondo, M. Tanabashi, and K. Yamawaki, Prog. Theor. Phys. **89**, 1249 (1993).
[40] K.-I. Kondo, H. Mino, and K. Yamawaki, Phys. Rev. D **39**, 2430 (1989); W. A. Bardeen, S. T. Love, and V. A. Miransky, Phys. Rev. D **42**, 3514 (1990).
[41] P. E. L. Rakow, Nucl. Phys. **B356**, 27 (1991).
[42] K.-I. Kondo, Int. J. Mod. Phys. A **06**, 5447 (1991).
[43] P. O. Bowman, U. Heller, D. Leinweber, M. Parappilly, A. Sternbeck, L. von Smekal, A. Williams, and J. Zhang, Phys. Rev. D **76**, 094505 (2007); A. C. Aguilar, D. Binosi, and J. Papavassiliou, Phys. Rev. D **86**, 014032 (2012); A. Ayala, A. Bashir, D. Binosi, M. Cristoforetti, and J. Rodríguez-Quintero, Phys. Rev. D **86**, 074512 (2012).